ARCHIVES OF CIVIL ENGINEERING, LVII, 4, 2011

DOI: 10.2478/v.10169-011-0027-z

FINITE ELEMENT MODELING OF COMPOSITE CONCRETE-STEEL COLUMNS

L. KWAŚNIEWSKI[1], E. SZMIGIERA[2], M. SIENNICKI[3]

This paper presents the numerical part of the research program on concrete-filled steel columns. Nonlinear, three dimensional FE analysis of axial compression, was conducted using the finite element program ABAQUS. The numerical results were validated through comparison with experimental data in terms of ultimate loading and deformation modes. Modeling related problems such as the definition of boundary conditions, imperfections, concrete-steel interaction, material representation and others are investigated using a comprehensive parametric study. The developed FE models will be used for an enhanced interpretation of experiments and for the predictive study of cases not included in the experimental testing.

Key words: concrete-filled battened steel columns; composite columns; finite element analysis.

1. Introduction

Composite concrete-filled steel columns are getting more and more attention in civil engineering practice due to the effective application of steel and concrete, leading to increased strength and stiffness comparing to other traditional solutions such as pure steel or reinforced concrete columns. There are a large number of studies on this topic involving analytical (Chen & Lin [3]), experimental (Chicoine *et al.* [4], Giakoumelis & Lam [9], Wang [18], Zoltowski *et al.* [19]) and numerical methods with experimental validation (Ellobody & Young [7], Johansson & Gylltoft [13], Liang *et al.* [15], Ding & Wang [6], Pan *et al.* [16], Gupta *et al.* [10]). Many researches are working on solutions which are simple and inexpensive and at the same time produce reliable structural members. There are investigated columns with and without reinforcement (Chen & Lin [3]), different cross-section shapes such as built-up shapes (Chen & Lin [3], Chicoine *et al.* [4]), concrete-filled square hollow section (SHS) (Ellobody & Young [7], Liang *et al.* [15]), and rectangular hollow section (RHS) (Wang [18], Ellobody & Young [7]),

[1] Professor, Department of Civil Engineering, Warsaw University of Technology, Warsaw, Poland, e-mail: l.kwasniewski@il.pw.edu.pl

[2] PhD., Department of Civil Engineering, Warsaw University of Technology, Warsaw, Poland, e-mail: e.szmigiera@il.pw.edu.pl

[3] PhD., Department of Civil Engineering, Warsaw University of Technology, Warsaw, Poland, e-mail: m.siennicki@il.pw.edu.pl

concrete filled tubes (CFT) (Giakoumelis & Lam [9], Johansson & Gylltoft [13], Ding & Wang [6], Gupta *et al.* [10]) or concrete encased H or I sections (Chen & Lin [3], Wang [18]). A method for estimation the ultimate strength of rectangular concrete-filled steel tubular (CFT) stub columns under axial compression is proposed by Huang et al. [12]. The ultimate strength of concrete core is determined taking into account a failure criterion of concrete under triaxial compression. Example material constitutive models for concrete-filled tube columns of circular cross section are proposed in (Hu et al. [11]). These models are implemented into the ABAQUS finite element program and verified against experimental data. In Lee [14] moment-curvature formulas are proposed for high-strength concrete filled square tube columns (HCFT), based on analytic assumption. The extensive subject literature review can be found in Chen & Lin [3] and Ellobody & Young [7].

Due to the novelty of these solutions the main objectives of this research are the estimation of ultimate loading and the prediction of failure mechanisms. An FE analysis accompanying a limited experimental study can be very helpful because of two reasons. First, large amount of numerical results and ease with their visualization help to interpret experimental results. Secondly, once validated the FE models can be easily modified and used for the parametric study and "what if" sensitivity analysis.

The columns considered here are the steel columns built from two I beams connected through welded batten plates and filled with concrete. In the existing standards, the computation and design of steel-concrete composite columns composed of compound steel sections is not sufficiently represented (Giakoumelis & Lam [9], Ellobody & Young [7]). It follows from engineering practice that this kind of columns might have wide application in the industrial buildings (Szmigiera *et al.* [17]). According to the authors' opinion there is the possibility to apply a composite action of this type of columns in the underground substructures, in the buildings erected using the "up & down" method or for strengthening steel columns in existing structures.

The FE analysis with the aid of a general purpose computer program was developed in this research to study the behavior of pure steel and concrete-filled steel columns subjected to gradually increasing axial loading. The paper describes comprehensively development of the FE models of the selected columns, and validation using the experimental results (Zoltowski *et al.* [19]). Modeling related problems such as the definition of boundary conditions, imperfections, concrete-steel interaction, material representation and others are investigated using a parametric study.

2. DESCRIPTION OF THE COLUMNS CONSIDERED

Considered here four columns, selected from a set of 23 experimentally tested are presented in Fig. 1 and described in Table 1. The only difference between columns A1 and A2 is the spacing of the batten plates (the same as between B1A1 and C1A2). Each of these configurations is considered in two versions, one version without concrete (A1

and A2) and one version with concrete (B1A1 and C1A2). All the steel components are made of the same steel grade S235JRG2.

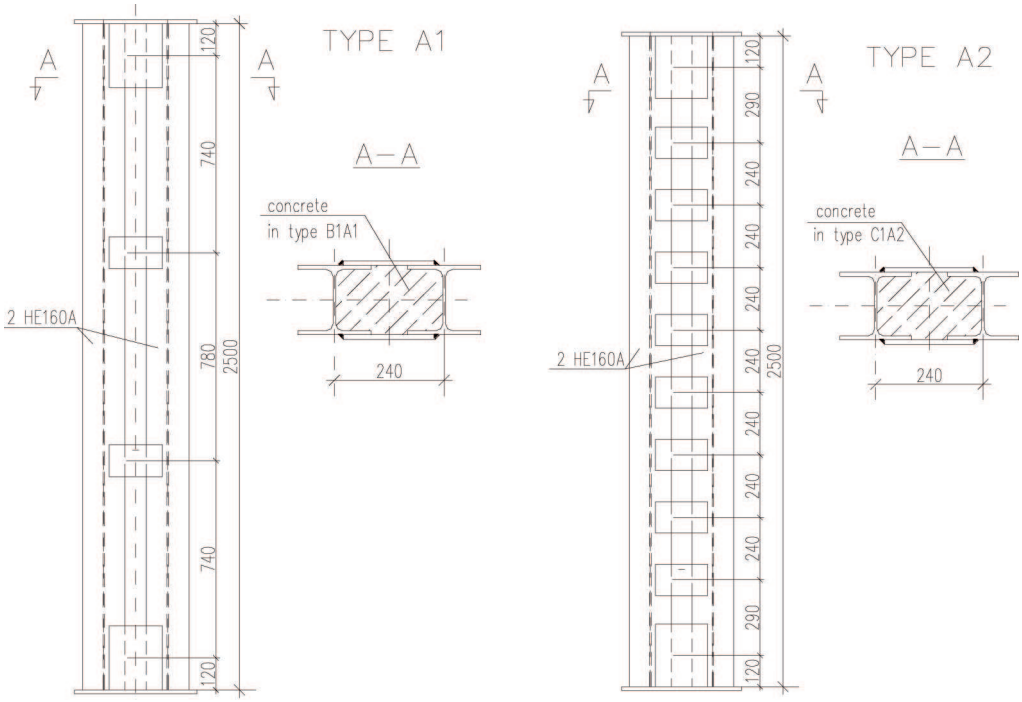

Fig. 1. Dimensions and cross-sections for tested columns.
Rys. 1. Wymiary i przekroje badanych słupów

Table 1

Properties and description of tested columns.
Właściwości i opis badanych słupów

Column	Materials	Batten spacing
A1	steel	780
A2		240
B1A1	steel filled with concrete class C20/25	780
C1A2		240

The column dimensions with the batten plates spacing are shown in Fig. 1. All batten plates are welded on the external side only.

During the experiments the columns were loaded axially in vertical position in the hydraulic test machine (Fig. 2). The bottom end plate, supported on a horizontal uniform surface, did not experience any vertical upward displacements indicating its

rotation. The loading was applied uniformly to the top end plate through a hinged solid slab.

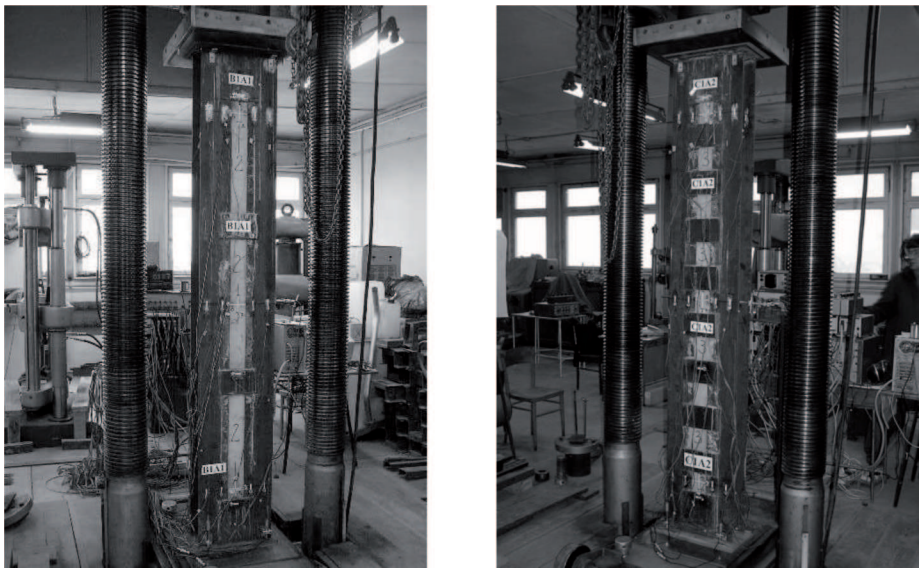

Fig. 2. Experimental test setup.
Rys. 2. Stanowisko badawcze

In addition to the ultimate load, the strains in concrete and steel, and displacements of selected points were measured. The measurements of longitudinal and transverse deformation of steel and concrete were made in three sections, using electrical strain gauges with gage lengths of 20 mm – for steel and 75 mm – for concrete. Deflection of columns in two planes and their longitudinal contraction were recorded using LVDT sensors.

After reaching the critical load the end plate started to rotate about its horizontal axis as shown in Fig. 7, 8, 9 and 10.

3. FINITE ELEMENT MODELS

3.1. GENERAL ASSUMPTIONS

To simulate the entire loading process, beyond the critical point, nonlinear analysis was conducted using general purpose, finite element program ABAQUS [1]. For the static analysis involving implicit solver the main problem encountered is usually premature termination due to lack of convergence. As it is shown below the success of calculation depends on selection of input parameters. The search for optimal setup is

not straightforward and should be well organized to avoid too many trail calculations. The logic is to move from simplest to more complex cases.

The FE model development was divided into two stages. In the first stage, a 3D model for column A1 was created and then a parametric study was conducted. The goal was to determine optimal model parameters for boundary condition representation, loading and imperfections, mesh density, element type, and analysis type and controls. The verification was done through comparison with the experimental data in terms of ultimate loading and post buckling deformation. In the second stage, a concrete core was added and a limited calibration process was conducted focusing on material properties of concrete and concrete – steel interaction. The developed FE models with determined parameters are described below. Some findings concerning parametric study are also presented.

3.2. GEOMETRY AND FE MESH

The FE models of columns were developed using geometric data shown in Fig. 1. As an example, the FE meshes for column A1 (Table 1), with two densities, are presented in Fig. 3. All steel components are modeled with four node shell elements with nodes located in the mid planes. Additionally, there is a rigid plate built of solid elements attached to the top end plate. The rigid plate is used in the FE models to transmit uniform loading to the top end of the column. After checking that different options for interaction between the rigid plate and the end plate do not affect results, the simplest solution was chosen for further calculations. The rigid plate was fully connected with the column through merged overlapping nodes.

The concrete core is modeled using solid elements. The mesh of the concrete core is divided into elements in such a way that external nodes coincide with nodes representing the steel components. All possible interactions can be traced by defining contact between concrete and steel components or by merging nodes.

In the first stage of the model development, a sensitivity study was conducted for column A1 to find proper element type selections. Finally S4R four-node shell elements were used for the steel parts and C3D8 eight-node solid elements for the concrete core. Different types of elements gave very similar results in this case.

To check if the original mesh density shown in Fig. 3 (on the left) was sufficient, calculations for the column A1 were repeated for a refined mesh with the number of elements increased 4 times (Fig. 3 on the right). The new model gave a very similar equilibrium path which exhibits difference only for large deformations, as shown in Fig. 4. The post buckling deformation pattern was similar.

3.3. LOADING AND BOUNDARY CONDITIONS

The calculations are supposed to simulate the test conditions as closely as possible. During the experiments, the columns were compressed in a hydraulic test machine

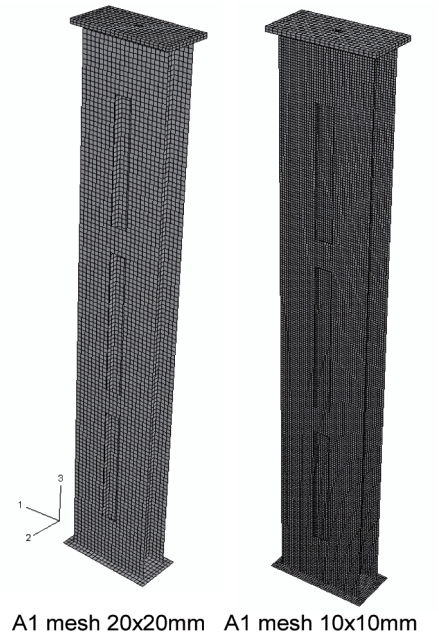

Fig. 3. Two FE meshes for column A1.
Rys. 3. Dwie siatki MES dla słupów A1

between two solid slabs. The slab on the top was hinged and the second one on the bottom was fixed. After reaching the critical load the top end plate started to rotate about its horizontal axis (as shown in Fig. 7, 8, 9 and 10).

To simulate contact between the columns and the bottom slab all external nodes in the column end plate have their vertical translations constrained. Additionally, a few nodes around the midpoint have two other translations constrained in order to remove some rigid body movements for the column. In this way the bottom end plate is partially fixed, it cannot rotate but most of it can expand freely in the horizontal directions.

As mentioned above, the plate built of solid elements is added to the FE model to transmit uniform loading to the top end of the column. This part is defined in the FE model as a rigid body accompanied with the reference point, located close to the midpoint on the top surface. Imperfection, in the form of load eccentricity, can be applied by moving the reference point from the midpoint location. The loading is applied through the reference point as a prescribed vertical displacement with horizontal displacements constrained. The loading defined as a prescribed displacement, monotonically growing, is especially suitable for nonlinear analysis, reaching beyond ultimate or critical loading when reaction forces decrease. The vertical reaction and displacement recorded for the reference point are used to formulate equilibrium paths (see Fig. 4, 5, 6, and 7). The loading coming from the rigid machine's slab is transfor-

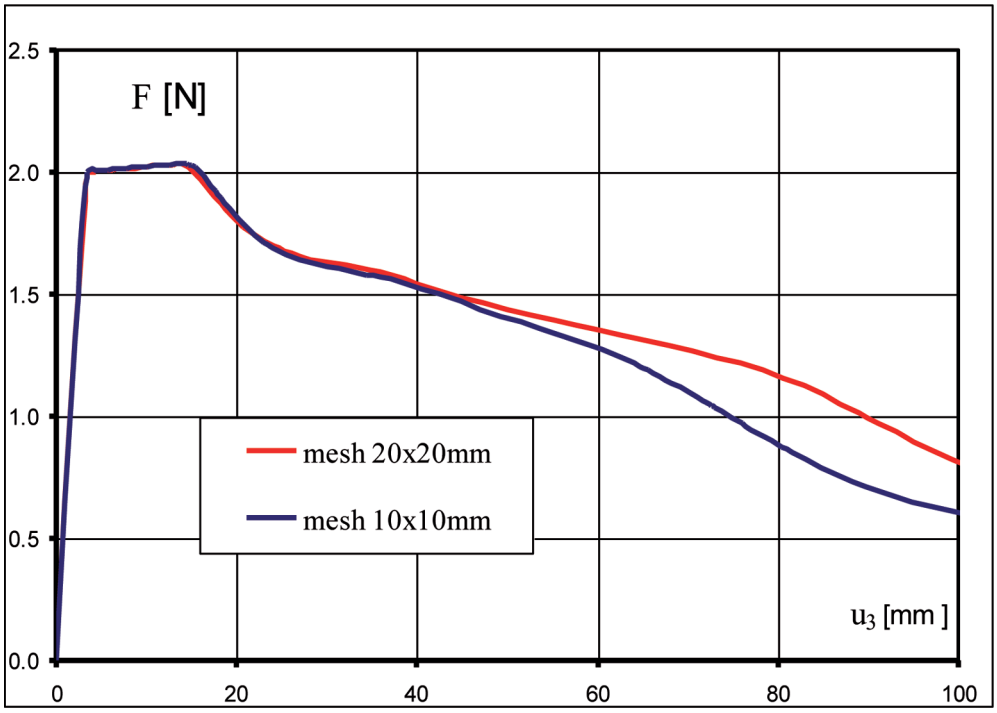

Fig. 4. Comparison of equilibrium paths for meshes shown in Figure 3.
Rys. 4. Porównanie ścieżek równowagi dla siatek pokazanych na rys. 3

med uniformly to the column's top end plate. This transmission can be realized in the FE model through contact definition or by merging coinciding nodes. Comparison of results showed that the overall performance of a column is the same. Merging nodes was chosen for further calculations as a simpler and more effective option.

3.4. MATERIAL PROPERTIES

To investigate numerically the post buckling behavior of the columns it is necessary to represent correctly the inelastic material properties in the FE models. The steel is modeled as an elastic-plastic material with isotropic hardening [1]. The Mises yield surface is defined by giving the value of the uniaxial yield stress as a function of uniaxial equivalent plastic strain. The input is based on the true stress – strain curve shown in Fig. 8. The first curve in Fig. 8 named "ABAQUS input" depicts the relation between true stress σ_T and true plastic strain ε_T^{PL} :

$$\varepsilon_T^{PL} = \varepsilon_T - \frac{\sigma_T}{E_s}. \tag{3.1}$$

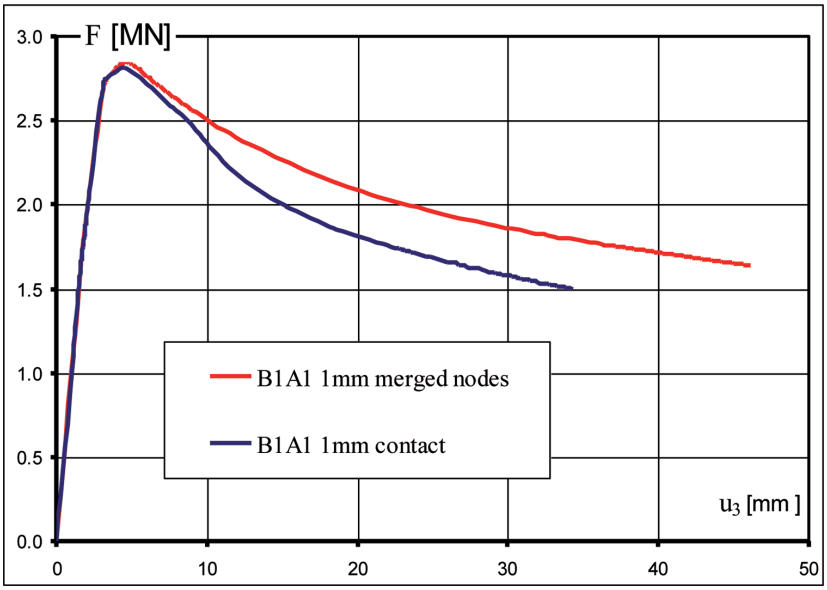

Fig. 5. Comparison of results for case B1A1 and two models, with contact and merged nodes.
Rys. 5. orównanie wyników dla przypadku B1A1 i dwóch modeli słupa: z kontaktem i z połączonymi węzłami

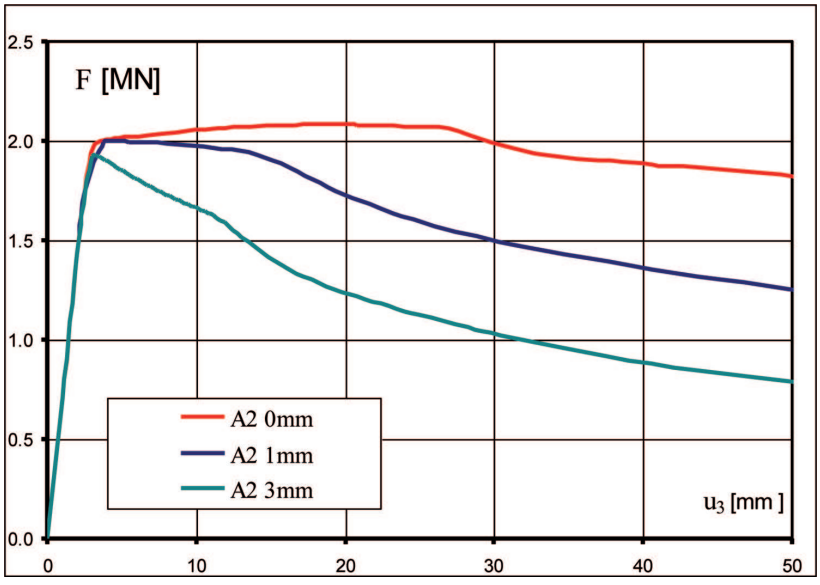

Fig. 6. Equilibrium paths for case A2 and three different locations of reference point.
Rys. 6. Ścieżki równowagi dla przypadku A2 przy trzech różnych położeniach punktu przyłożenia obciążenia

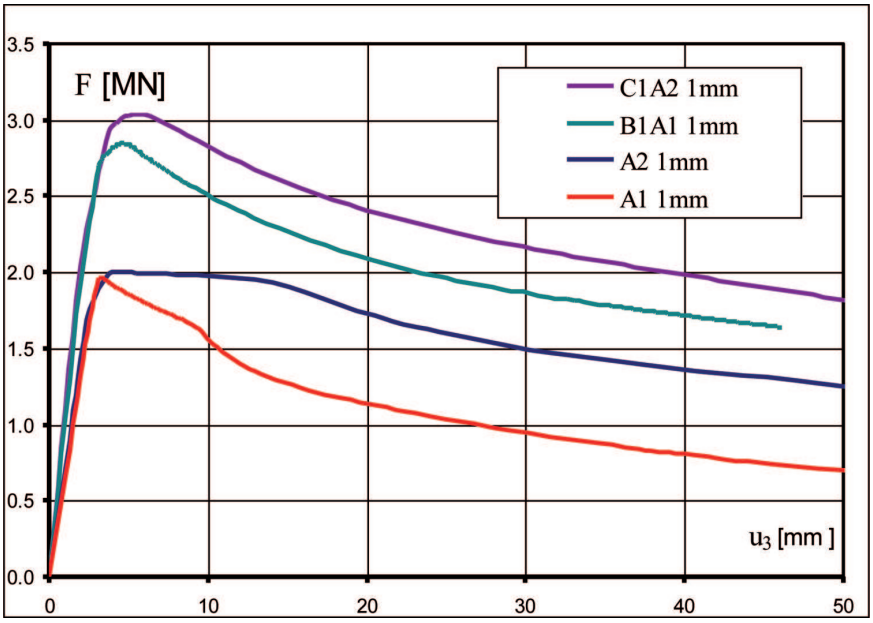

Fig. 7. Calculated equilibrium paths for eccentricity e=1mm.
Rys. 7. Obliczone ścieżki równowagi dla mimośrodu e=1mm

where E_s is the elastic modulus (see Table 2). This curve directly defines the plastic properties in the FE model. That relation is approximated by a limited number of points shown in Fig. 8.

The diagrams in Fig. 8 show two stress–strain curves for the steel. The first, engineering curve σ_E-ε_E was obtained from coupon tests. The second, true stress-strain curve σ_T-ε_T, was calculated using the following formulas (from [1]):

$$\sigma_T = \sigma_E(1 + \varepsilon_E), \tag{3.2}$$

$$\varepsilon_T = \ln(1 + \varepsilon_E). \tag{3.3}$$

Experimentally determined basic material properties for the steel and the concrete are presented in Table 2.

The parametric study conducted for the case A1 showed that a more precise relationship, with many points, causes numerical problems leading to very small increments and very long calculations or even to program termination. Repeated calculations for different numbers of points defining the $\sigma_T - \varepsilon_T^{PL}$ relationship showed that the results are not affected unless all the points lay on the original curve $\sigma_T - \varepsilon_T$. The most critical is the first point defining the yield stress, especially for the ultimate loading approximation.

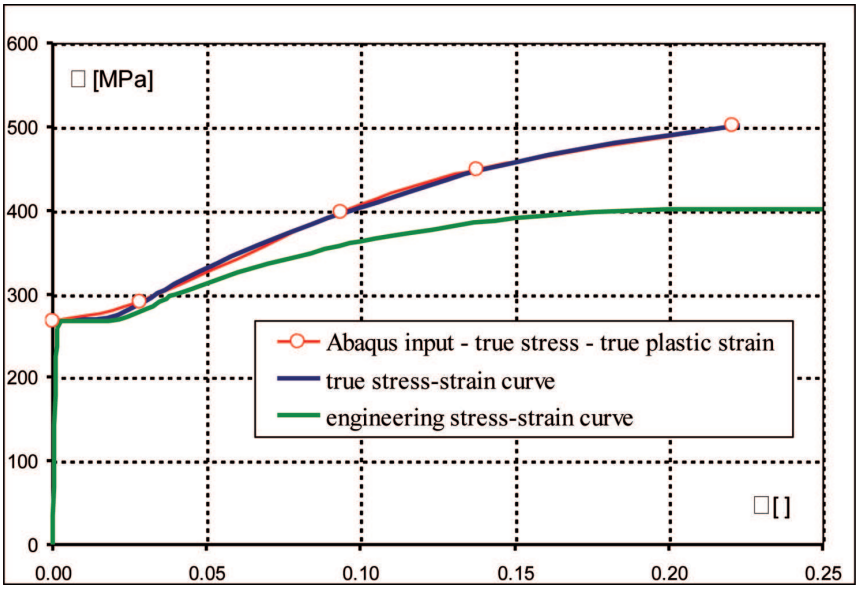

Fig. 8. Stress – strain curves for steel S235JRG2.
Rys. 8. Wykresy zależności naprężenie-odkształcenie dla stali S235JRG2

Table 2

Basic material properties for steel and concrete.
Podstawowe właściwości stali i betonu

Steel S235JRG2		Concrete C20/25	
Elastic modulus E_s	205 GPa	Elastic modulus E_{c0}	27.4 GPa
Poisson ratio ν_s	0.3	Poisson ratio ν_c	0.18
Yield stress σ_{sY}	267 MPa	Yield stress σ_{cY}	17.29* MPa
Ultimate stress σ_{sU}	401 MPa	Crushing failure stress σ_{cU}	31.7 MPa
* approximated values based on ABAQUS Example Problems Manual, (2006)		Plastic strain at failure ε_{cF}	0.0015*
		Cracking failure stress σ_{cT}	2.8 MPa

In ABAQUS, complex, inelastic materials can be modeled by combining different material behaviors. The elastic behavior of concrete is assumed to be isotropic and linear. The inelastic concrete behavior is modeled using model *Concrete Damaged Plasticity with two sub options *Concrete Compression Hardening, and *Concrete Tension Stiffening [1]. It is recommended for plain and reinforced concrete [1]. This model uses concepts of isotropic damaged elasticity in combination with isotropic tensile and compressive plasticity to represent the inelastic behavior of concrete and other brittle materials. The concrete damaged plasticity model is based on the assumption of isotropic damage. The degradation of the elastic stiffness is induced by plastic straining both in tension (cracking) and compression (crushing). For tension beyond

the failure stress the micro-cracking is represented macroscopically by softening in the stress-strain response. For uniaxial compression the response is linear up to the value of initial yield, σ_{cY}, then the plastic response is typically characterized by stress hardening followed by strain softening beyond the ultimate stress, σ_{cF}. Table 2 includes applied material data for steel and concrete coming from tests on cast cylinders and also approximated using proportions taken from [2].

3.5. SOLUTION PROCEDURE

The calculation involves one step of a static stress analysis. Due to high nonlinearities at local and global levels, accompanying the traced inelastic, unstable, collapse and postbuckling behavior, Riks analysis was chosen as the solution [1]. The Riks method is based on the concept of arc length as a measure of the solution progress in load-displacement configuration space. The load, defined here as a prescribed displacement, is an additional unknown. The solution proceeds incrementally along the static equilibrium path, providing loads and displacements which satisfy equilibrium equations with acceptable tolerance. The increments are established automatically by the program. The user specifies only initial, minimum and maximum increments and termination criterion. The magnitude of an increment depends on the number of iterations and attempts, needed in the previous increment.

For nonlinear problems, as the one described here, the solutions are depended on the magnitude of increments. Although usually they follow initially the same equilibrium path, very often the solution near the critical point experiences problems with convergence and premature termination. For all cases considered here the fast and proper solution was obtained for the default set of analysis parameters and a limited number of points defining inelastic material response. Smaller initial increments or more detailed stress-strain curves led to long calculations and premature termination.

3.6. CONCRETE – STEEL INTERACTION

Fig. 5 presents two equilibrium paths for the two FE models of the column B1A1. The models represent two extreme solutions for modeling concrete – steel interaction. In the first model the meshes for the concrete core and steel components are not connected and there is frictionless one way contact defined. In the second model both meshes are fully connected through merged nodes. Fig. 5 shows that there is little difference between the results. It confirms findings in [13] where different setups for tubes filled with concrete were tested. For concrete cores inclosed by steel sheets on all sides (top and bottom) there is little relative displacement on the interfaces at the beginning of loading. The relative large deformation is captured by concrete tensile softening.

3.7. LOADING IMPERFECTION

Imperfections are always present in actual tests and can be considered in the FE analysis in different ways. Most common is to apply geometrical imperfections as a combination of eigenfunctions obtained from a linear buckling analysis. The disadvantage of this solution is that location of plastic zones can be dependent on which eigenfunction was selected to modify the initial location of the nodes. In the present work the imperfection was applied as a loading eccentricity. Fig. 6 presents three equilibrium paths for the column A2 and three different locations of the reference point where the prescribed displacement (loading) was applied. The considered positions of the reference point are e=0, 1, and 3 mm along $y(2)$ axis (Fig. 6). The comparison of the results shows small reductions in the critical load and visible change in location of plastic zones as shown in Fig. 9, especially for e=0mm.

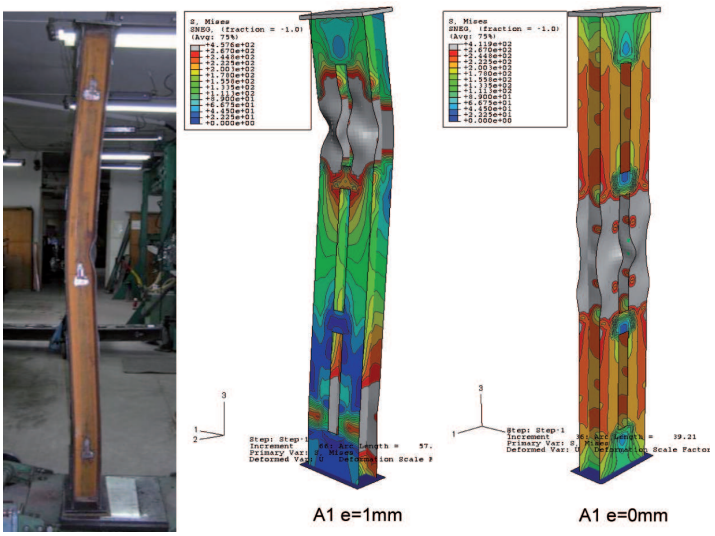

Fig. 9. Comparison of actual and simulated deformation for column A1.
Rys. 9. Porównanie rzeczywistego i obliczonego odkształcenia słupa A1

Table 3 presents comparison of ultimate loading, calculated and experimentally determined for all four columns. These magnitudes are compared with the theoretical maximum F_{MAX} expressed as a sum of maximum compression strengths of steel section A_s and concrete section A_c (without reduction due to buckling):

$$F_{MAX} = \sigma_{sU} A_s + \sigma_{cU} A_c, \tag{4.1}$$

where ultimate stresses σ_{sU} and σ_{cU} are given in Table 2. Fig. 7 presents corresponding equilibrium paths, calculated for an eccentricity e=1mm. All calculated ultimate loads are smaller than the actual values. The main reason for the discrepancy are the boundary

conditions on the top end plates. In the FE models the ideal boundary conditions do not capture actual moments which are non zero due to friction. Fig. 9, 10, 11 and 12 show a comparison of the deformation for the FE models and the experiments. Presented states were obtained in the post buckling range, for approximately the same total column's contraction of 30 mm. For each case with the concrete filling three specimens were used in the tests. Although all the experimental magnitudes of the ultimate loading were close there were sometime different deformation configurations. The comparison of these configurations exhibits some similarities with the numerical results, for cases with loading eccentricities. It should be remembered that in the actual columns there are also geometric and material imperfections as a result of welding.

Table 3

Calculated and experimentally determined ultimate loading F_U and efficiency F_U/F_{MAX}.
Obliczeniowe i otrzymane z badań maksymalne obciążenie F_U oraz stosunek F_U/F_{MAX}

	Experiment		FEA		Maximum
Column	F_U	F_U/F_{MAX}	F_U	Difference Experiment vs. FEA	F_{MAX} (4)
	[kN]	[%]	[kN]	[%]	[kN]
A1	2160	69	1965	9.0	3112
A2	2140	69	1997	6.6	3112
B1A1	3060	74	2728	10.8	4152
C1A2	3333	80	3013	9.6	4152

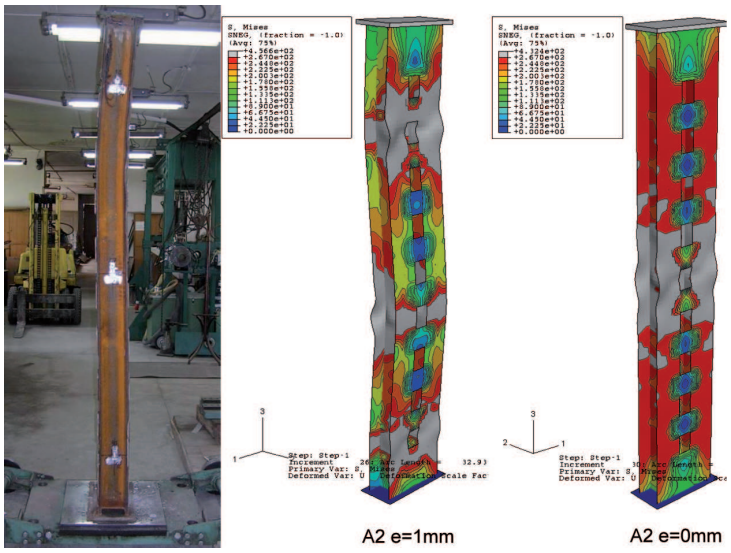

Fig. 10. Comparison of actual and simulated deformation for column A2.
Rys. 10. Porównanie rzeczywistego i obliczonego odkształcenia słupa A2

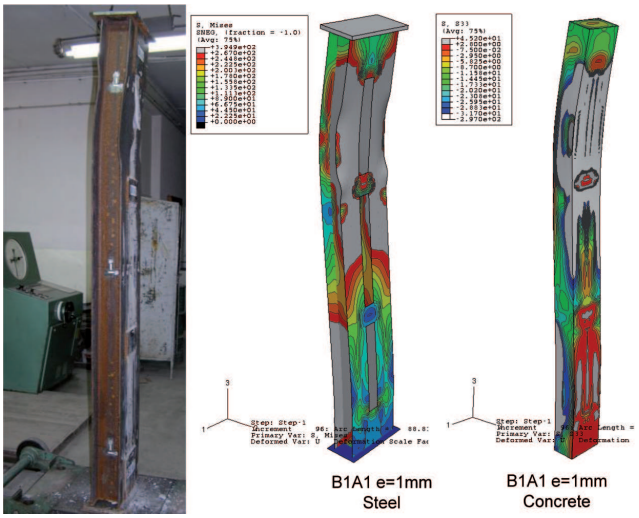

Fig. 11. Comparison of actual and simulated deformation for column B1A1.
Rys. 11. Porównanie rzeczywistego i obliczonego odkształcenia słupa B1A1

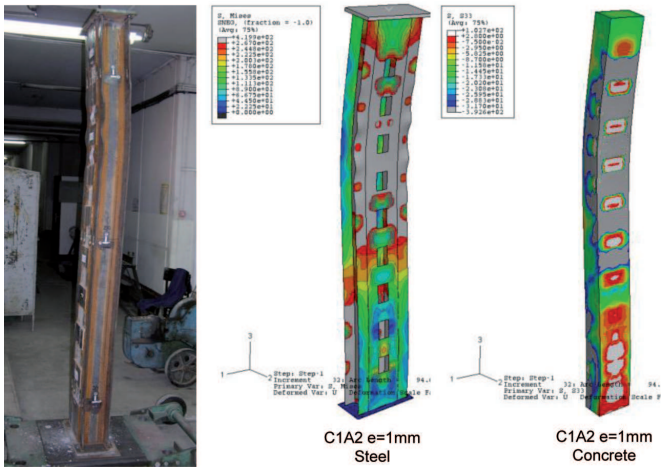

Fig. 12. Comparison of actual and simulated deformation for column C1A2.
Rys. 12. Porównanie rzeczywistego i obliczonego odkształcenia słupa C1A2

4. SUMMARY AND CONCLUSIONS

The paper is focused on the FE model development of steel columns with a concrete core. The main objective of this part of the research was to accurately simulate the

actual tests and to identify which model parameters can reasonably affect the results. Based on the conducted parametric study and comparison with the experiments the following conclusions were formulated for the considered FE models:

1. A variation of the interaction between concrete and steel does not substantially affect the results.

2. To avoid numerical problems the inelastic material response should be approximated by curves with a limited number of points. The magnitude of the yield stress is critical for ultimate load estimation. The effect of residual stresses due to welding of the side plates was not taken into account in the presented research.

3. Imperfections in the form of loading eccentricity do not reduce the ultimate load significantly but can change the deformation pattern. This explains the variation of deformation obtained in the experiment. The effect of imperfections highlights the importance of precise measurements before testing to evaluate the actual geometrical imperfections.

4. The effectiveness of the conducted calculations involving Riks analysis were dependent on analysis parameters determining the magnitudes of increments.

5. Smaller numerical estimates of ultimate capacity are caused by idealization of boundary conditions.

Although the numerically determined ultimate loading was underestimated, the comparison of the FE analysis with the experiment investigation was found to be satisfying in terms of both, loading and deformation prediction.

AKNOWLEDGEMENTS

The study reported in this paper is supported by a grant from the Polish Ministry of Science and Higher Education titled: ”Determination of load capacity of steel concrete composite columns with battened steel sections”. The authors would like to express their appreciation for this generous support. Opinions and views expressed in this paper are those of the authors and not necessarily those of the sponsoring Agency.

REFERENCES

1. ABAQUS Analysis User's Manual, ABAQUS, Inc., Version 6.6-1, USA 2006.
2. ABAQUS Example Problems Manual, ABAQUS, Inc., Version 6.6-1, USA 2006.
3. C.-C. CHEN, N-J. LIN, *Analytical model for predicting axial capacity and behavior of concrete encased steel composite stub columns*, Journal of Constructional Steel Research, **62**, 424-433, 2006.
4. T. CHICOINE et al., *Behavior and Strength of Partially Encased Composite Columns with Built-up Shapes*, Journal of Structural Engineering, March, 279-288, 2002.
5. T. CHICOINE, MASSICOTTE, R. TREMBLAY, *Long-Term Behavior and Strength of Partially Encased Composite Columns Made with Built-up Shapes*, Journal of Structural Engineering, February, 141-150, 2003.

6. J. DING, Y.C. WANG, *Realistic modeling of thermal and structural behaviour of unprotected concrete filled tubular columns in fire*, Journal of Constructional Steel Research, **64**(10), 1086-1102, 2008.
7. E. ELLOBODY, B. YOUNG, *Nonlinear analysis of concrete-filled steel SHS and RHS columns*, Thin-Walled Structures, **44**, 919-930, 2006.
8. Eurocode 4, *Design of composite steel and concrete structures*. Part 1.1 General rules for buildings, 2004.
9. G. GIAKOUMELIS, D. LAM, *Axial capacity of circular concrete-filled tube columns*, Journal of Constructional Steel Research, **60**, 1049-1068, 2004.
10. P.K. GUPTA, S.M. SARDA, M.S. KUMAR, *Experimental and computational study of concrete filled steel tubular columns under axial loads*, Journal of Constructional Steel Research, **63**(2), 182-193, 2007.
11. H.-T.HU, F.-C. SU, M. ELCHALAKANI, *Finite element analysis of CFT columns subjected to pure bending moment*, Steel & Composite Structures, October, **10**(5), 415-428, 2010.
12. Y.-S. HUANG, Y.-L. LONG, J. CAI, *Ultimate strength of rectangular concrete-filled steel tubular (CFT) stub columns under axial compression*, Steel & Composite Structures, April, **8**(2), 115-128, 2008.
13. M. JOHANSSON, K. GYLLTOFT, *Mechanical Behavior of Circular Steel-Concrete Composite Stub Columns*, Journal of Structural Engineering, **14**(5), 491-508, 2002.
14. S.-J. LEE, *Capacity and the moment-curvature relationship of high-strength concrete filled steel tube columns under eccentric loads*, Steel & Composite Structures, April, **7**(2), 135-160, 2007.
15. Q.Q. LIANG, B. UY, R. LIEW, *Nonlinear analysis of concrete-filled thin-walled steel box columns with local buckling effects*, Journal of Constructional Steel Research, **62**, 581-591, 2006.
16. J.L. PAN, T. XU, Z.J. HU, *Experimental investigation of load carrying capacity of the slender reinforced concrete columns wrapped with FRP*, Construction and Building Materials, **21**(11), 1991-1996, 2007.
17. E. SZMIGIERA, W. ZOLTOWSKI, M. SIENNICKI, *Research on load capacity of concrete filled columns with battened steel sections*, Journal of Civil Engineering and Management, **16**(3), 313-319, 2010.
18. Y.C. WANG, Tests on slender composite columns, Journal of Constructional Steel Research, **49**, 25-41, 1999.
19. W. ZOLTOWSKI, E. SZMIGIERA, M. SIENNICKI, *The influence of concrete filling steel columns with two battened chords on their behavior*, Proceedings of 8^{th} International Conference on Steel, Space & Composite Structures, Kuala Lumpur, Malaysia, May, 15-17, 2006.

NUMERYCZNE MODELOWANIE ZESPOLONYCH SŁUPÓW STALOWO-BETONOWYCH

S t r e s z c z e n i e

W artykule przedstawiono numeryczną część programu badań słupów stalowych wypełnionych betonem. Przeprowadzono nieliniową, trójwymiarową analizę FE ściskania osiowego, za pomocą programu ABAQUS. Numeryczne wyniki zostały zwalidowane przez porównanie z danymi doświadczalnymi w zakresie obciążenia granicznego i typu odkształcenia. Za pomocą kompleksowych studiów parametrycznych badano zagadnienia związane z modelowaniem takich parametrów jak określenie warunków brzegowych, imperfekcji, interakcji między betonem a stalą, odwzorowaniem materiałów. Opracowane modele FE zostaną wykorzystane do udoskonalenia interpretacji eksperymentów i przewidywania wyników dla przypadków niebadanych doświadczalnie.

Remarks on the paper should be sent to the Editorial Office no later than March 31, 2012

Received September 14, 2011 revised version December 15, 2011